Motion of Aromatic Hydrocarbons in the Microporous Aluminum Methylphosphonates AlMePO-α and AlMePO-*β*

Jorge Gonzalez,[†] R. Nandini Devi,[†] Paul A. Wright*,[†] David P. Tunstall,[‡] and Paul A. Cox[§]

School of Chemistry, University of St. Andrews, St. Andrews, Fife, United Kingdom, KY16 9ST, School of Physics and Astronomy, University of St. Andrews, Fife, U.K., KY16 9SS, and School of Pharmacy and Biomedical Science, University of Portsmouth, Portsmouth, United Kingdom, PO1 2DT

Received: May 17, 2005; In Final Form: August 26, 2005

^{2}H wide-line NMR has been used, in conjunction with molecular dynamics simulations where appropriate, to follow the reorientation of the monoaromatic compounds benzene, toluene, and *p*-xylene within the one-dimensional channels of the α- and *β*-polymorphs of aluminum methylphosphonate, $Al_2(CH_3PO_3)_3$. Variable-temperature, static, ^{2}H NMR spectra of adsorbed d_6-benzene, d_3-, d_5-, and d_8-toluenes, and d_3,d_3-*p*-xylene were matched by line shape simulation. The motion of *p*-xylene in both polymorphs is approximated by the long axis of the molecule describing a cone within the channels, the half-angle of which is greater for the slightly wider channels in AlMePO-*β* (27−30° cf. 18−19°). The ^{2}H NMR of d_3-toluene is simulated using a similar model, whereas the signal from aromatic deuterons in d_5- and d_8-toluenes is simulated by a ring undergoing $2\pi/3$ flips around the para axis. The reorientation of benzene shows the largest differences between the two pore structures. In AlMePO-*β* it tumbles with little restriction, although at low temperatures the spectral details are better matched by allowing the molecule to spend a greater proportion of its time closer to the wall. In AlMePO-α the much broader line shape arises from constrained motion within the strongly triangular channels. Molecular dynamics simulations of benzene in the two structures confirm the differences. They support a model for benzene in AlMePO-α where its motion is restricted to rotations about its 6-fold axis and $2\pi/3$ jumps between symmetry-related sites in the pores, so that the plane of the aromatic ring remains approximately parallel to the *c*-axis.

Introduction

The discovery of the extended family of microporous organic−inorganic hybrid solids holds great promise for the development of materials for gas storage and separation, with selectivities that can be tailored according to the size and polarity of the target molecule. Such hybrid organic−inorganic microporous molecular sieves can be divided into two classes, one comprising metal−organic frameworks or "MOFs" and the other including solids with an inorganic "skeleton" lined with organic groups. The former can be envisaged as metal or metal oxide nodes linked by organic ligands, such as di-or tricarboxylates or amines,[1−3] giving a wide variety of frameworks that may have very high free volumes. The latter family typically includes metal phosphonates, in which the three phosphonate oxygens link into the inorganic framework and the organic groups extend into the pore space. There are fewer porous structures of this type, and the pores are typically smaller, but there are some that possess microporous frameworks.[4]

Two of the most interesting and completely characterized solids of the latter type are the aluminum methylphosphonates AlMePO-α and AlMePO-*β* of Maeda et al.[5,6] These are closely related polymorphs of composition $Al_2(CH_3PO_3)_3$ that contain hexagonal arrays of one-dimensional channels that are lined with methyl groups and have free diameters of around 6 Å (Figure 1). The internal surfaces have been shown to impart to the solid very different gas adsorption properties from those of purely inorganic zeolitic solids. In particular, the solids show type V isotherms for the adsorption of H_2O as a result of their hydrophobicity.[7] Furthermore, the characteristic triangular shape of the pore in the α-polymorph results in a stepped isotherm for nitrogen,[7] which can be simulated by atomistic modeling to reveal a well-ordered packing configuration of the N_2 molecules within the pores at higher loadings.[8] The pore sizes of these AlMePOs are similar to those of ZSM-5 type zeolites that are known to show strong shape-selective effects in the adsorption and separation of xylene isomers. The origin of this selectivity has been elucidated in part by wide-line ^{2}H NMR spectroscopy and subsequent peak shape analysis.[9−11] ^{2}H NMR spectroscopy has been shown to be a powerful tool to address the nature of hydrocarbon−zeolite interactions.[12] As an example of the importance of adsorbate mobility, Denayer et al.[13] have recently shown that the rotational mobility of molecules in medium-pore zeolites plays an important part in the effects of "inverse shape selectivity" in which branched alkanes that are able to rotate are retained more strongly than linear alkanes that cannot.

In this work, we have used ^{2}H NMR methods to measure the mobility of the monoaromatic hydrocarbons benzene, toluene, and *p*-xylene within the two AlMePO polymorphs to determine the effective free space for these molecules and the constraints on molecular motion that the pores exert. ^{2}H NMR has recently been used successfully to investigate the motion of d_6-benzene included within coordination polymers.[14−16] Where the molecular motion of a ^{2}H-containing molecule is constrained, the NMR peak shape of a static sample is broader than the narrow line expected for isotropic motion (random tumbling). If the motion can be approximated by a relatively

[†] School of Chemistry, University of St. Andrews.
[‡] School of Physics and Astronomy, University of St. Andrews.
[§] University of Portsmouth.

10.1021/jp052590z CCC: $30.25
Published on Web 10/26/2005

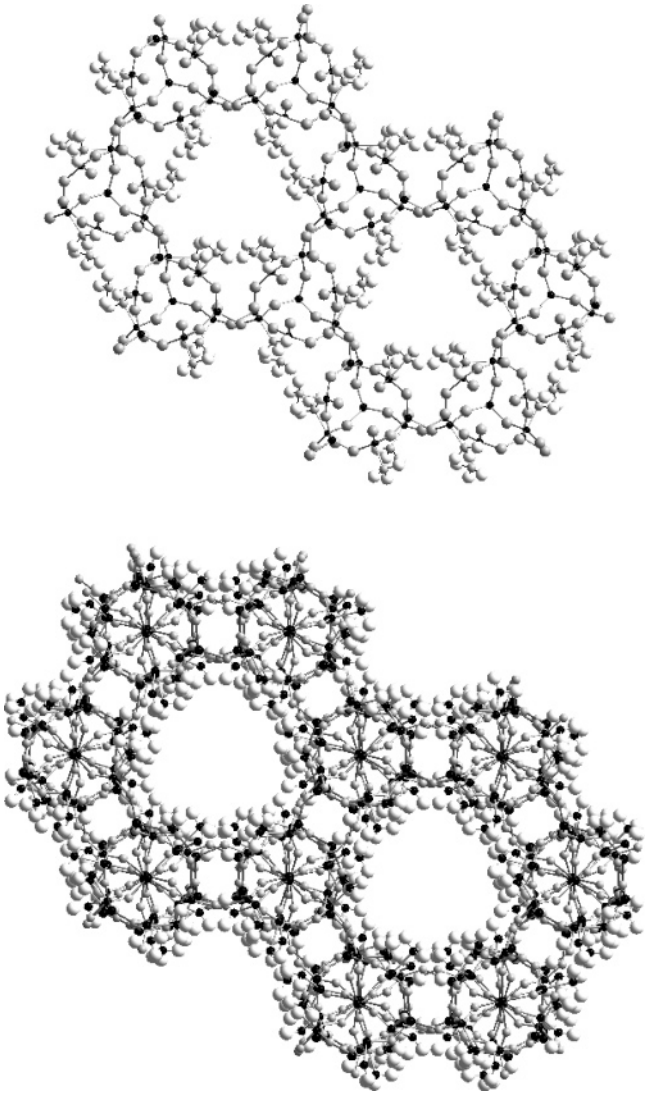

Figure 1. Structures of AlMePO-α (top) and AlMePO-β (bottom), viewed down the one-dimensional channel axes. Note that the pore cross section is much more markedly triangular in AlMePO-α. The channels are lined with methyl groups.

simple geometric model, it is possible to simulate the experimental line shape. Several computer programs are available that are able to perform these simulations—in this study we use the program MXQET.[17,18] The MXQET computer code permits the calculation of ^{2}H NMR spectra for molecules performing complicated motion by expressing the reorientation in terms of rotations of C−D bonds within frames of reference that are defined in the input. Where different mechanisms of reorientation occur for the same C−D bonds, these can be simulated by inclusion of a separate set of rotations in another reorientational frame in the input. Finally, if different sets of deuterons are present, the final spectrum will be a combination of the signals, although the integrated intensities will not be directly proportional to the number of deuterium nuclei if their T_2 relaxation behavior is strongly divergent. The MXQET program has been applied successfully to adsorption in zeolites,[19] to inclusion in hybrid solids,[16] and also to problems of biological relevance.[20]

Models for the motion that give rise to simulated spectra that match the observed ^{2}H NMR may not be unique, so use must be made of known constraints of the molecule and the geometric relationship of molecule and pore when proposing models for the reorientation. For very rapid motion it is also possible to propose models of motion within the pores on the basis of molecular dynamics (MD) simulations (bearing in mind that even long MD runs only cover time scales on the order of 10^{-9} s). We therefore performed MD calculations on guest−host systems studied in this work to help resolve ambiguities in the line shape simulation. Molecular dynamics simulations have previously been shown to give great insight into the mechanisms of hydrocarbon motion within microporous solids.[21]

Here we report the temperature-dependent ^{2}H NMR spectra of deuterated benzene, toluene, and *p*-xylene within the pores of AlMePO-α and -β. Neither *p*-xylene nor toluene is small enough to rotate completely within the channels of either polymorph, so the freedom with which they can reorient about their long axes is found to be very sensitive to the channel dimensions. Furthermore, the rotation of the aromatic ring about the para-axis is in these cases monitored by the use of appropriately deuterated molecules. Benzene is very close in size to the dimensions of the channels, and the deuterium NMR of C_6D_6 discriminates strongly between the similar channel structures of the two solids, which permit free tumbling within β but not in α. The details of the very different motion of benzene in the two pore systems are analyzed by a combination of experimental ^{2}H NMR measurements and theoretical MD simulations, emphasizing the power of a joint experimental and theoretical approach to analyzing hydrocarbon motion.

Experimental Section

Several batches of AlMePO-β were prepared according to the published procedure.[6−8] Typically, aluminum hydroxide (Aldrich, 98%) and 1,4-dioxane (Avocado, 98%) were added to an aqueous solution of methylphosphonic acid (Aldrich, 98%) in the molar ratio $Al(OH)_3$:$CH_3PO_3H_2$:$C_4H_8O_2$:H_2O = 1:1.5:0.5:40. The mixture was stirred until homogeneous and heated in a PTFE-lined stainless steel autoclave for 48 h at 433 K. The product was filtered and dried at 333 K overnight. 1,4-Dioxane was removed from the pores by heating under flowing dry nitrogen at 723 K for 12 h.

AlMePO-α was prepared by topotactic transformation of as-prepared AlMePO-β under a rapid flow of nitrogen saturated with water vapor, according to the procedure described independently by Carter et al. and Maeda et al.[22] The temperature was raised at 10 K/min to 773 K and kept at this temperature for 8 h. It was also possible to prepare AlMePO-α directly by hydrothermal synthesis, but the products of these experiments were found to show very low adsorption capacities for hydrocarbons, and so were not used.

Samples of AlMePO-β and -α were characterized by X-ray powder diffraction (XRD), ^{27}Al and ^{31}P MAS NMR, and toluene adsorption. X-ray diffraction was performed using a Stoe Stadi/p diffractometer operating in transmission geometry with monochromated Cu $K\alpha_1$ radiation (λ = 1.540 56 Å). ^{31}P and ^{27}Al MAS NMR studies of the as-prepared samples were performed on a Varian Infinityplus 500 MHz spectrometer, with a standard Chemagnetics 4 mm probe. Samples were spun at the magic angle at a speed of 10 kHz. Pulse durations were 1.0 and 4.0 μs and pulse delays were 0.2 and 1.0 s for ^{27}Al and ^{31}P, respectively. Adsorption measurements were made gravimetrically using a fully automated Hiden IGA instrument.

For the ^{2}H NMR experiments the solid was loaded to a depth of 20 mm into specially adapted glassware consisting of a Pyrex glass NMR tube (5 mm in diameter) attached to a Schlenk tube. The samples were degassed under vacuum on a glass line at 423 K, which was sufficient to remove all water molecules. A known amount of the deuterated organic molecule was dosed onto the solid from the vapor phase, with the constraint that all

of the adsorbate would be within the pores. The sample tubes were partially immersed in liquid nitrogen to ensure no organic vapor pressure was present before sealing the other end of the glass tube with a flame. Into each AlMePO polymorph were loaded 1.5 wt % d_3,d_3-*p*-xylene, 4.5 wt % d_3-, d_5-, and d_8-toluenes, and loadings of both 1.5 and 4.5 wt % d_6-benzene.

^{2}H NMR spectra were collected using a Varian Infinityplus solid state NMR operating at 500.15 MHz for ^{1}H (76.78 MHz for ^{2}H) using a static solenoid Bruker probe. The quadrupole echo pulse sequence ($90°_x-\tau-90°_y-\tau$-echo) was used, where the latter half of the echo signal was acquired and Fourier transformed. The 90° pulse was 3.6 μs. Spin−lattice relaxation times were measured using a saturation recovery method followed by a quadrupole echo sequence for the acquisition, i.e., $(90°)_n-\tau_0-90°_x-\tau-90°_y-\tau$-echo, $n \geq 40$. T_1 values were calculated from exponential fits of the evolution of the area of the signal as a function of the time τ_0. Low-temperature experiments were performed using cold nitrogen gas produced by evaporating liquid nitrogen from a tank connected to the probe, controlling the temperature of the sample with a heater, and monitoring the temperature with a thermocouple on the sample chamber of the probe.

The ^{2}H NMR spectra were simulated through the MXQET and MXQET1 codes. The latter possesses the option to include environments across which the entire molecule can exchange on the NMR time scale. In these simulations, values taken for the quadrupolar coupling constants were 168 kHz for aliphatic C−D deuterons (deduced from the experimental spectum of phosphonate $-CD_3$ groups within deuterated AlMePO-β[23]) and 193 kHz for aromatic deuterons.[24] Models for reorientation are described in the text: angles for rotations and exchange rates were varied in the program to match the experimental spectra as closely as possible. Initial checks confirmed that the program accurately reproduced wide-line spectra measured for well-defined molecular motions described in the literature with the appropriate reorientation models.

Molecular dynamics calculations were performed using the CVFF force field as implemented in the program Discover.[25] Simulations were performed for 5000 iterations to allow the system to equilibrate prior to a final production run of 100 000 iterations using a time step of 1×10^{-15} s, giving a simulation time of 1×10^{-10} s for analysis. Charges for the framework were derived from a density functional theory optimization of the two AlMePO frameworks.[26] The inorganic part of the AlMePO frameworks was held fixed during the simulations, but the CH_3 groups lining the channels were allowed to rotate. The coordinates of the organic molecule were stored every 500 iterations during the production run prior to subsequent analysis. The MD simulations were performed at a theoretical temperature of 298 K, but were taken to be representative of the types of motion possible at lower temperatures as well.

Results and Discussion

Characterization of the Samples. X-ray diffraction (Figure 2), ^{31}P NMR (Figure 3), and ^{27}Al NMR (not shown) indicate that the AlMePO-β is pure, with the pattern and spectrum being as reported, without additional reflections or resonances. Upon heating the as-prepared sample of AlMePO-β in nitrogen saturated with water vapor at 773 K, it is clear from the XRD and the ^{31}P NMR that the AlMePO-β has very largely converted to AlMePO-α. There are some weak reflections from unconverted starting material in the XRD, and weak signals in the ^{31}P and ^{27}Al NMR (the latter not shown) that are due to AlMePO-β. Integration of the ^{31}P signal suggests that the β content is around 5%. Although phase pure AlMePO-α could be prepared directly according to the method of Maeda,[7] in which a solid plug of alumina was heated in the presence of the methylphosphonic acid but in the absence of 1,4-dioxane, it was found to possess blocked pores, so the sample prepared by transformation was used for all of the ^{2}H NMR experiments on molecular mobility.

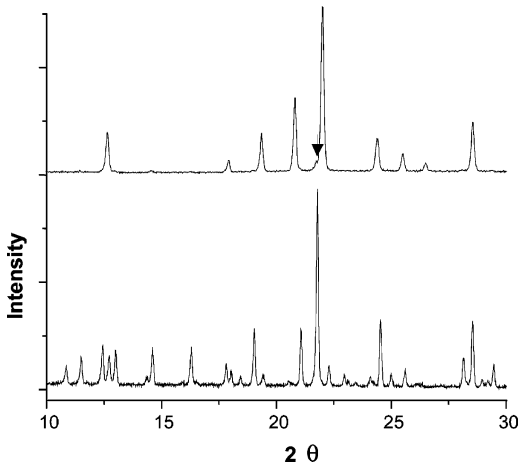

Figure 2. XRD patterns from 10° to 30° 2θ of (below) as-synthesized AlMePO-β and (above) AlMePO-α prepared from β by heating in nitrogen saturated with water vapor. The main reflection from unreacted β is arrowed.

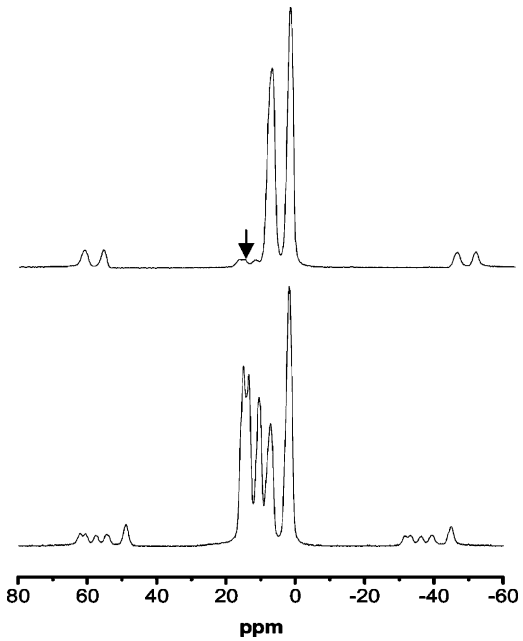

Figure 3. ^{31}P MAS NMR of (below) as-prepared AlMePO-β and (above) AlMePO-α prepared from β. Resonances from unreacted β are arrowed.

The adsorption isotherms for toluene at 298 K (taken to be a representative probe of porosity accessible to the aromatics investigated in this study) show that both the AlMePO-α and -β samples can adsorb over 6 wt % (Supporting Information). On this basis, all of the adsorbates used in this work (benzene, toluene, and *p*-xylene) were adsorbed well below the level of pore filling and so will be adsorbed within the pores and not on the external surfaces.

^{2}H Quadrupolar Echo NMR Studies.

d_3,d_3-p-Xylene in AlMePOs-β and -α. The wide-line ^{2}H spectra and interpreted dynamics of the *p*-xylene molecules are discussed first because the modes of reorientation of this

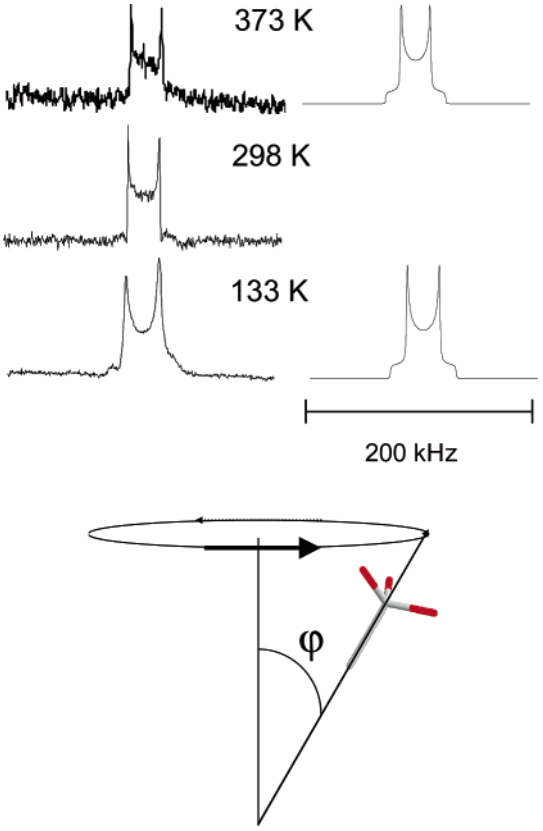

Figure 4. Quadrupole echo ^{2}H NMR spectra of d_3,d_3-*p*-xylene in AlMePO-β (left). It can be simulated assuming fast motion of the para-axis around three sites on a cone and associated rapid clicking of the CD_3 group around its axis (bottom) to give a good match (right) for cone half-angles of 30° at 373 K and 27° at 133 K.

molecule are very strongly constrained in the unidimensional channels of the AlMePO polymorphs and consequently the spectra are straightforward to analyze. Only the d_3,d_3-isotopomer was examined, since the main aim of this series of experiments was to determine the effective free diameter of the channels as experienced by *p*-xylene.

d_3,d_3-p-Xylene in AlMePO-β. The ^{2}H spectra for the labeled *p*-xylene are typical so-called Pake doublets, uniaxial powder patterns with sharp edges, over the entire temperature range studied (Figure 4). The distance between the "horns" increases from 26 to 29 kHz as the temperature is decreased from 373 to 133 K. Because a methyl ($-CD_3$) group clicking only about its C_3 axis (at the fast limit of motion) would produce a spectrum where these features were separated by 42 kHz, the molecule must be undergoing additional motion in relation to the aluminophosphonate framework. The most likely type of motion, given the geometry of the molecule−channel complex and the line shape of the signal, is that the *p*-xylene is moving so that its long axis is moving between different sites on a cone. MXQET simulations, in which the half-angles of the cone of motion are varied to match the observed spectra, predict that the cone's half-angle decreases from 30° to 27° over the temperature range examined (Figure 4). These simulations are independent of the number of sites (>2) used to describe the motion of the molecule's long axis around the cone.

d_3,d_3-p-Xylene in AlMePO-α. The spectra recorded for d_3,d_3-*p*-xylene adsorbed on the AlMePO-α sample are shown in Figure 5. Over most of the temperature range studied, the spectra appear as a superposition of two Pake doublets with different widths. Noticeably, one set of signals has the same peak-to-peak separation as that observed for AlMePO-β, so this was

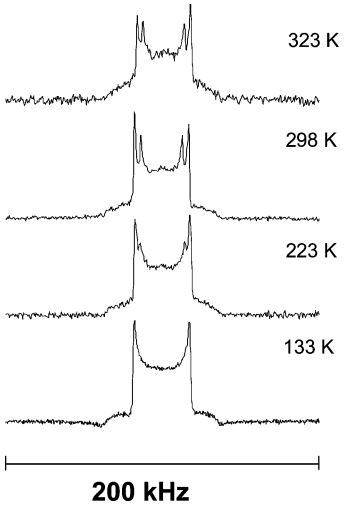

Figure 5. Quadrupole echo ^{2}H NMR of d_3,d_3-*p*-xylene adsorbed in AlMePO-α.

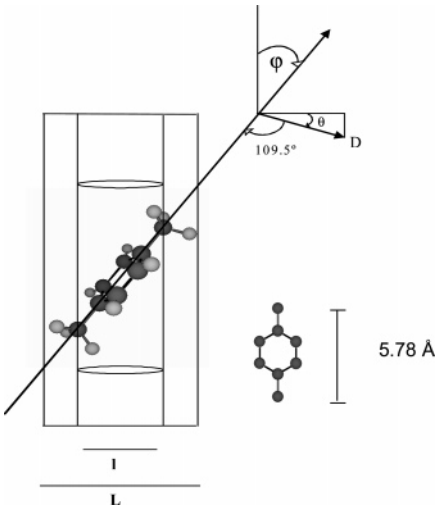

Figure 6. Diagrammatic sketch used to estimate the free diameter of one-dimensional channels from cone angles of d_3,d_3-*p*-xylene used in simulating ^{2}H NMR. *I* is the C(sp^3) to C(sp^3) distance of *p*-xylene projected across the pores, φ the half-angle of the cone of rotation, and $\theta = \varphi - 19.5°$, used in trigonometric calculation of the free diameter, *L*.

attributed to signal from *p*-xylene adsorbed in the small amount of unconverted AlMePO-β. Although it is not possible to quantify accurately the two signals, it appears that the *p*-xylene adsorbs preferentially onto the larger pore AlMePO-β at the higher temperatures, because the relevant ^{2}H signal is larger than expected on the basis of the ^{31}P NMR of the amount of unreacted β. The signal attributed to *p*-xylene in AlMePO-α is broader, with peak-to-peak separations increasing from 34.5 kHz (at 298 K) to 35.5 kHz (at 133 K). These line shapes can be simulated by allowing the long axis of the *p*-xylene to move between sites on cones with half-angles of 19° and 18°, respectively.

The results show that ^{2}H NMR of the d_3,d_3-*p*-xylene molecule is a sensitive probe of the channel dimensions in AlMePO-β and -α. The spectra are readily simulated by a model for the motion where the long axis moves around a cone. Using a simple geometric model (Figure 6) where the motion inscribes a cylinder, and taking typical C−C and C−D bond lengths and van der Waals radii of deuterium atoms, the mean pore diameters are estimated at 7.3 Å for AlMePO-β and 6.2 Å for AlMePO-α. The discrepancy from crystallographic estimates of 6.0 and

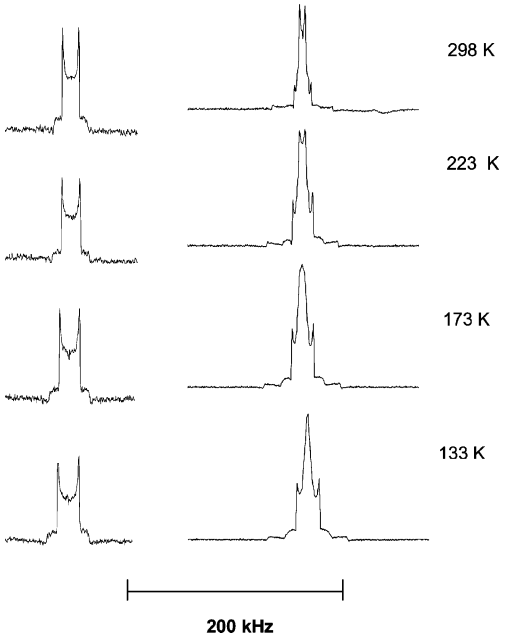

Figure 7. Variable-temperature quadrupole echo ^{2}H NMR of d_3-toluene (left) and d_8-toluene (right) adsorbed in AlMePO-β.

5.3 Å, respectively, is likely to arise partly because no account is taken in the crystallographic measurement of deviations of the pore from a perfect cylinder. This ^{2}H NMR approach is suggested as a promising method for the estimation of the pore geometry of microporous solids of unknown structure.

Toluene in AlMePO-β and AlMePO-α. Toluene was chosen as a smaller aromatic molecule than *p*-xylene, but one that would still be unable to tumble freely within the pores. As well as investigating the reorientation of the molecule by analyzing the NMR signal from the methyl group (as $-CD_3$ in d_3-toluene), the motion of the aromatic ring was studied by using d_8-toluene (fully deuterated) and d_5-toluene (in which only the aromatic ring is deuterated).

Toluene in AlMePO-β. The deuterium quadrupolar echo spectra from d_3- and d_8-toluenes adsorbed in AlMePO-β at temperatures from 133 to 298 K are shown in Figure 7. The spectra of d_3-toluene contain direct information about the motion of toluene about its para-axis. Uniaxial powder patterns with sharp edges are observed at all temperatures, indicating that there is only one dynamic state. The width of the signals increases from 18 to 24 kHz as the temperature decreases from 298 to 133 K. The line shapes can be simulated using a similar motion around a cone that was employed for *p*-xylene, again taking the motion of $-CD_3$ groups around their C_3 axis to be in the fast limit ($>1 \times 10^9$ Hz) and reorienting the para-axis of the toluene at three sites on a cone. The cone half-angle that enables successful matching of the spectra decreases from 38° at 298 K to 32° at 133 K (Figure 8).

The spectra recorded on d_8-toluene in AlMePO-β result from the superposition of signals from the methyl groups, the aromatic deuterons in ortho and meta positions (strong signal), and the aromatic para to the methyl group (a weak, broad, signal). The signal from the aromatic deuteron in the para position has a width that varies from 65 to 82 kHz upon cooling from 298 to 133 K. The signal is consistent with that from a single deuteron exchanging between three sites on cones with the same angles as those determined by analysis of the d_3-toluene spectra. The remaining signal from d_8-toluene arises from the aromatic deuterons in ortho and meta positions. At 298 K this takes the form of a narrow double peak signal 7 kHz wide; this broadens

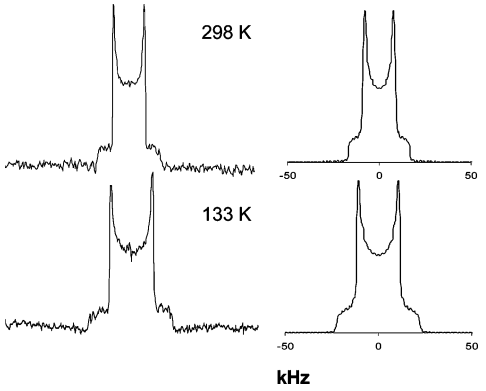

Figure 8. Experimental (left) and simulated (right) quadrupole echo ^{2}H NMR of d_3-toluene adsorbed in AlMePO-β at 133 and 298 K.

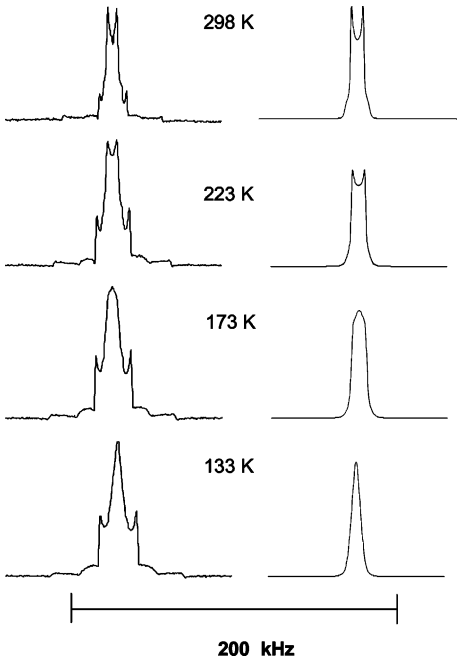

Figure 9. (left) Variable-temperature quadrupole echo ^{2}H NMR of d_8-toluene adsorbed in AlMePO-β. (right) Simulated spectra of the aromatic deuterons in the meta and ortho positions.

and changes shape as the temperature is decreased, until it becomes triangular with a full width at half-maximum height (half-width) of 8 kHz at 133 K. To simulate this signal, the aromatic ring was permitted to exchange between three positions, related by rotations of 120° ($2\pi/3$), to reflect the 3-fold rotation symmetry of the AlMePO-β channels (the structure has space group *R*3*c*). This motion is executed by molecules undergoing exchange between three sites on a cone, as described previously for *p*-xylene. Using this model, it was possible to simulate the line shapes of the signals due to the ortho- and meta-deuterons by additional $2\pi/3$ rotations with an exchange rate that decreased from 7×10^6 Hz at 298 K to 5×10^5 Hz at 133 K (Figure 9 and Table 1).

Combining all the simulated spectra gives the simulated d_8-toluene spectra (Figure 10). Using an Arrhenius plot (ln(frequency) vs $1/T$) to analyze the frequencies of exchange required to simulate this part of the d_8-toluene signal gives an activation energy of 5.3(8) kJ/mol for aromatic group rotation.

Toluene in AlMePO-α. The ^{2}H NMR spectra of d_3-, d_5-, and d_8-toluenes adsorbed in AlMePO-α at a loading of 4.5 wt %, and measured with a 35 μs delay between 90 pulses, are given in Figure 11. For d_3-toluene, the low-temperature data (133 K)

TABLE 1: Half-Angles of Cones of Reorientation Described by the Para-Axis of Toluene in AlMePO-α and AlMePO-*β*, and Exchange Rates of the Aromatic Deuterons about the Para-Axis, as Obtained by Matching the ^{2}H NMR of Deuterated Toluene from 123 to 298 K

	T/K	cone half-angle/deg	exch rate of arom deuterons/Hz
AlMePO-α	298	29	NA[a]
	223	25	NA[a]
	173	24	7.0×10^5
	133	22	NA[b]
AlMePO-*β*	298	38	7.0×10^6
	223	35	3.0×10^6
	173	33	1.4×10^6
	133	32	5.0×10^5

[a] Two dynamic states present. [b] Strongly attenuated echo signal not matched by MXQET.

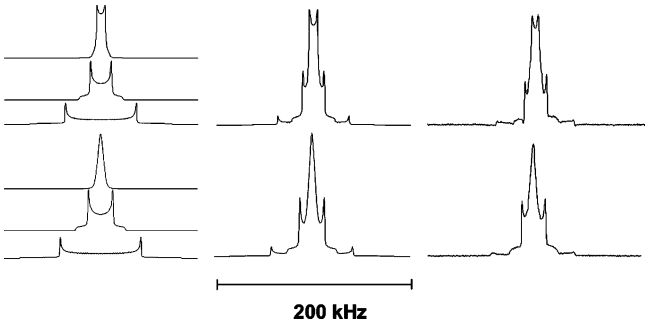

Figure 10. (left) Simulated components of aromatic and aliphatic deuterons of d_8-toluene in AlMePO-*β*, (center) summed simulated components of spectra, and (right) experimental spectra collected at 133 (below) and 223 K (above).

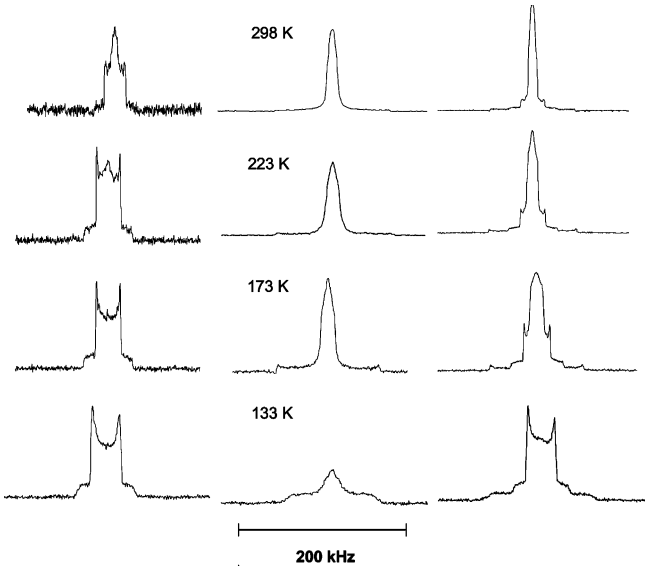

Figure 11. Variable-temperature quadrupole echo ^{2}H NMR of d_3-toluene (left), d_5-toluene (center), and d_8-toluene (right) adsorbed in AlMePO-α.

display a uniaxial powder pattern with 32 kHz separation between the horns. As the temperature is raised, the uniaxial signal remains, its width decreasing to 27 kHz at 298 K, but in addition at each temperature there is a very small signal from d_3-toluene adsorbed in unreacted AlMePO-*β*, and at 223 K and above a third signal is observed. This last signal, which grows in strength as the temperature is increased, takes the form of a triangular shape centered at zero frequency, with a half-width of 8 kHz. This indicates that more than one dynamic state is present at these temperatures, so that MXQET was not used to model these spectra. The single signal from d_3-toluene at 133 and 173 K indicates that there is only one dynamic state for toluene in AlMePO-α at these temperatures. The signal can be simulated by the toluene moving so that its long axis exchanges between different sites on a cone, as was the case for AlMePO-*β*. The shape of the channels in AlMePO-α is markedly triangular, so the line shape was simulated by the toluene molecule moving over three sites on the cone, with a half-angle that changes from 22° at 133 K to 29° at 298 K (Supporting Information). The additional signal that appears at higher temperatures is less readily modeled. It is thought to represent a separate dynamic state (or collection of states) and can be simulated by toluene executing jumps with large cone half-angles (between 48° and 52°).

The signal from d_5-toluene yields information on the reorientation of the aromatic ring. The broad signal that is observed derives from the deuteron para to the methyl group, and the observed widths are simulated by the same motion around a cone that is proposed to account for the spectra of d_3-toluene in AlMePO-α. The signal at 173 K from the aromatic deuterons ortho and meta to the methyl group was successfully simulated using a model similar to that used for toluene in AlMePO-*β*, namely a $2\pi/3$ reorientation of the aromatic ring within the AlMePO-α channels, with an exchange rate estimated from the MXQET program. This motion is apparent from considerations of molecular dynamics simulations (not shown), in which the plane of the molecule is observed to flip by 120° between sites within the channel, which has a clearly triangular cross section in α (Figure 1). Reduction in temperature to 133 K results in a strong decrease in the signal from d_5-toluene, and it was not possible to model this signal using the MXQET program. This echo attenuation suggests that the rotational exchange of the aromatic ring about its para-axis occurs at an intermediate exchange rate at this temperature ($\sim 10^5$ Hz). The d_8-toluene spectra closely match the summed d_3- and d_5-toluene signals, illustrating that the experiments are self-consistent.

In summary, ^{2}H quadrupole echo NMR of toluene in the AlMePOs indicates that the observed spectra can in large part be simulated by considering the para-axis of the toluene to exchange between at least three sites on a cone within the channels, while the aromatic ring undergoes an independent $2\pi/3$ flip around the long axis of the molecule. The details of the fit parameters used in the MXQET program to successfully match the observed spectra are summarized in Table 1. An additional high-temperature dynamic state of toluene in AlMePO-α has also been observed, and is attributed to toluene molecules, the para-axes of which are undergoing larger jumps (ca. 50° half-angles). Molecular dynamics studies of toluene (not shown) are consistent with the models for motion proposed to simulate the ^{2}H NMR, although inspection of the trajectories of toluene indicates that those models are idealized.

Benzene in AlMePO-α and -*β*. d_6-Benzene was chosen as a molecular probe because of its simplicity and its closeness in kinetic diameter to the channel dimensions of the AlMePOs. The ^{2}H NMR spectra within the two polymorphs show remarkable differences.

Benzene in AlMePO-β. The spectra of benzene, loaded at 1.5 and 4.5 wt % within AlMePO-*β* (corresponding to one molecule every 33 and 11 Å along the channels, respectively), were measured from 133 to 315 K. Similar behavior is observed at the two levels of loading: the line shapes at room temperature and above are isotropic (ca. 1 kHz wide), whereas cooling below this gives a narrow doublet, the half-width of which increases

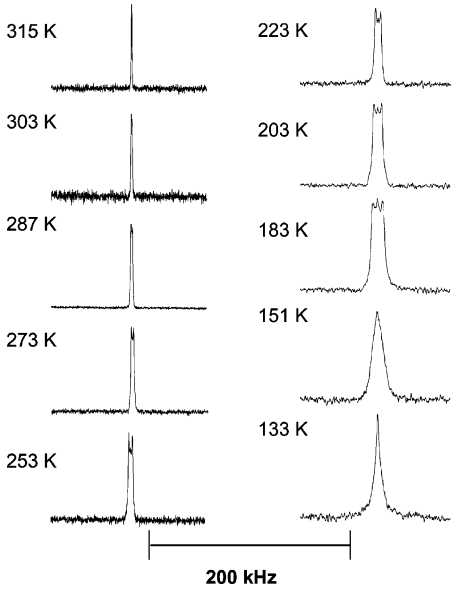

Figure 12. Variable-temperature quadrupole echo ^{2}H NMR of d_6-benzene adsorbed in AlMePO-β at a loading of 1.5 wt %. The motion is isotropic at 303 K and above. Upon cooling the spectral width (in kHz) increases: 287 (K), 1.8; 273, 2.3; 253, 3.1; 223, 5.1; 203, 7.0; 183, 10.0; 151, 15.0; 133, 7.0.

to around 10 kHz at 183 K (see Figure 12 for 1.5 wt % spectra). At 151 K and below the line shape is triangular. These spectra indicate that benzene moves rapidly in AlMePO-β and that at the higher temperatures undergoes isotropic tumbling in the pores. Measurements of T_1 made at these higher temperatures follow an Arrhenius relationship, in a plot of ln T_1 vs $1/T$, that gives an activation energy of 13.1(3) kJ/mol for the isotropic motion.

Molecular dynamics simulations also indicate that benzene can rotate freely (Figure 13), but they suggest that it occupies sites near the channel walls between these free rotations (for snapshots of these two situations, see the Supporting Information). Therefore, to explain the signal broadening upon lowering the temperature, the spectra were simulated by assuming the benzene can occupy two different sites: one in the center of the channel, with free rotation, and the second close to the wall, where it can spin about its C_6 axis. For the first site the quadrupolar coupling constant (QCC) is 0; for the second, it is 96.5 kHz. Assuming a fast exchange between the two sites, in a way similar to that proposed for the motion of cyclohexane in zeolite L,[19] the effective QCC is the weighted average of the two QCCs. Taking into account that the spectral width is 0.75 QCC, the relative populations of molecules in the two sites can be estimated for those signals that show a twin-horned line shape (Table 2).

At lower temperatures a triangular peak shape is observed, with a reduction in the half-width. Since lowering T will not result in increased mobility, the peak shape was modeled (Figure 14) using a ratio of populations extrapolated from higher temperature data and assuming exchange between the sites with intermediate exchange frequencies (frequencies of 4.5×10^5 and 5.0×10^4 Hz at 151 and 133 K, respectively). In the intermediate exchange rate, the ^{2}H NMR line shapes are known to be sensitive to the delay in the quadrupole echo pulse sequence. A series of experiments was therefore performed in which this delay was varied from 12 to 312 μs, and the simulated spectra were calculated using these values for the delay. The close agreement with experiment (Supporting Information) further supports this model of benzene dynamics at low temperature in AlMePO-β.

Benzene in AlMePO-α. ^{2}H NMR spectra of the AlMePO-α sample loaded with 4.5% benzene are shown in Figure 15. Over most of the temperature range, the spectra represent a superposition of two components, corresponding to benzene in two dynamic states. The narrow signal corresponds to C_6D_6 exhibiting isotropic behavior, and is attributed to benzene molecules adsorbed on unreacted AlMePO-β. The main signal, from benzene on AlMePO-α, is a uniaxial powder pattern above 200 K and triangular below this temperature.

The ^{2}H line shapes indicate that benzene does not exhibit isotropic motion in the constrained channels of AlMePO-α, but there is still considerable anisotropic motion leading to line narrowing. Activation energies, derived for the d_6-benzene in AlMePO-α from the temperature dependence of T_1, were 7.0 and 9.8 kJ mol^{-1} for loading levels of 1.5 and 4.5 wt %, respectively. It is expected that rotation about the C_6 axis will be one component of the motion, but additional modes must be present. Molecular dynamics simulations suggest that the benzene molecule flips so that the plane of the molecule rotates by $2\pi/3$ between sites within the strongly triangular-shaped channels (Figure 13). The ^{2}H NMR spectra simulated by this combination of rotations and flips, both at the fast limit of motion, reduces the QCC to 46.5 kHz, still larger than that observed. Closer inspection of the MD simulations suggests that the benzene wobbles while in the channels, so that fast $\pi/6$ out-of-plane motion was included in the MXQET model. This gives a Pake doublet with a separation of 17 kHz, matching that observed experimentally at 323 K and above (Figure 16).

At lower temperatures, the line shape changes to triangular. The spectrum at 153 K can be matched by using the same dynamic model as before, but using an intermediate exchange rate of 5×10^5 Hz for the "clicking" of the benzene around its C_6 axis. The exchange rate used to describe the $2\pi/3$ flips of the benzene molecule with respect to the framework was again taken as being in the fast limit. Finally, the line shape at 123 K, half-width 20.8 kHz, could, after many attempts at simulation using the MXQET program, be fitted most closely by using exchange rates of 2×10^6 Hz for the $2\pi/3$ flips and 4.8×10^4 Hz for the C_6 rotation.

Summary of Motion of Benzene in AlMePOs. The contrasting dynamic modes and ^{2}H wide-line quadrupole echo spectra for C_6D_6 benzene in the two AlMePO polymorphs illustrate the ability of the technique to differentiate between pore systems of closely similar dimensions and chemical characteristics. In AlMePO-β, the benzene undergoes isotropic motion down to the lowest temperatures measured, as well as spending a relatively small fraction of its time at the walls of the channels. This very high mobility, which is greater than that observed on cationic zeolites such as Na−X or Na−Y,[21] or on the large pore metal−organic framework MOF-5,[16] is likely to be a consequence of the rapidly rotating methyl groups that line the channels and are most closely in contact with the adsorbate. Although the internal surfaces in AlMePO-α are similar, the more restricted channel space, which is strongly triangular in shape, prevents isotropic reorientation, and the benzene molecules exchange between sites in which the plane of the rotating aromatic rings remain approximately parallel to the channel axis. This constraining effect of the pores of AlMePO-α has been shown previously to give interesting effects in the adsorption of N_2 molecules, as a result of constrained modes of packing.[7,8] The experimentally observed tumbling motion of d_6-benzene in AlMePO-β is predicted by theoretical MD simulations.

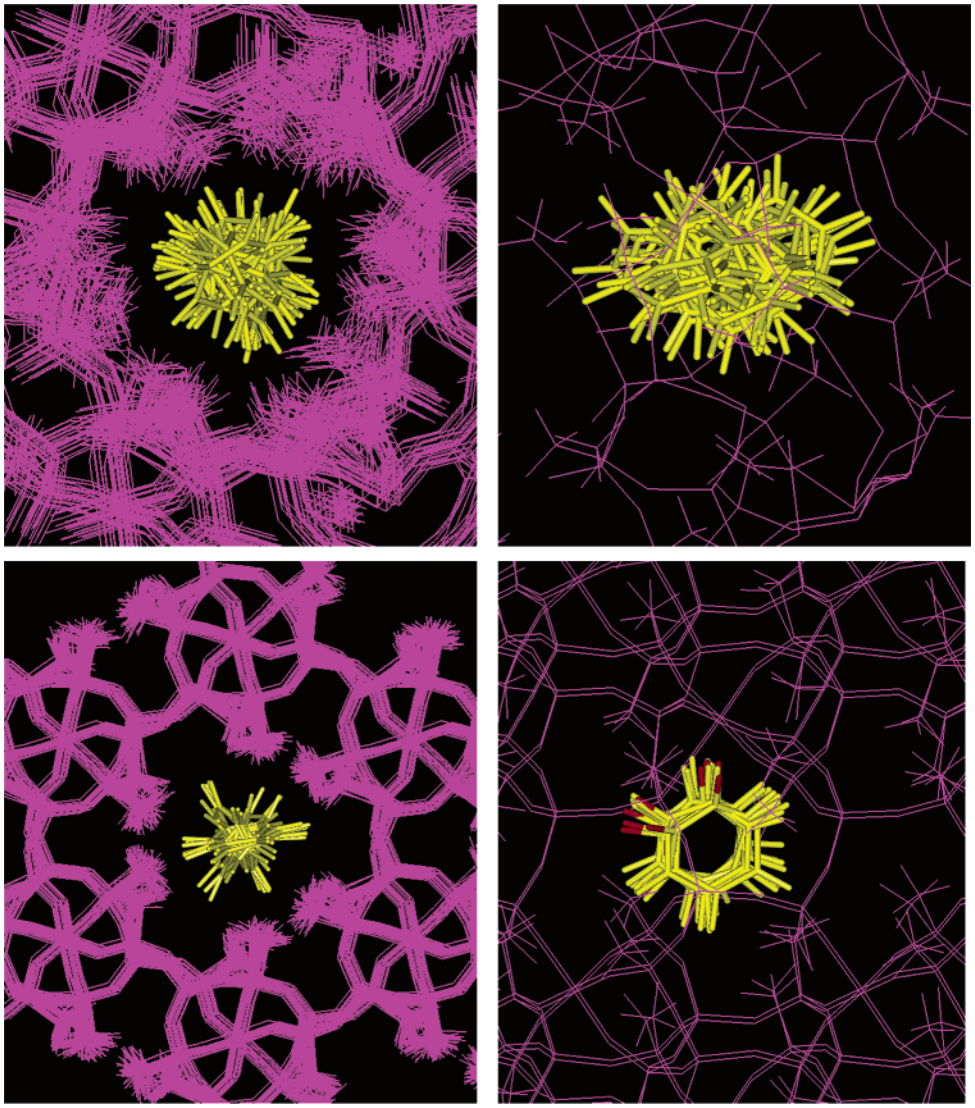

Figure 13. Trajectory of benzene molecules within the pores of (above) AlMePO-β and (below) AlMePO-α. The structure is viewed along the channel axes (left) and perpendicular to these axes (right). The location of benzene in AlMePO-α is shown every 2.5×10^{-12} s for the full length of the 1×10^{-10} s simulation. The location of benzene in AlMePO-α is shown every 5×10^{-12} s during the full 1×10^{-10} of the simulation. The orthogonal view of the motion of benzene in AlMePO-α is shown every 5×10^{-13} s between 1.25×10^{-11} and 1.70×10^{-11} s. One of the hydrogen atoms has been colored red to show its position during this period.

TABLE 2: Estimate of the Fractional Site Occupancies of Benzene Rotating Isotropically (N_{iso}) and Located at the Wall Sites (N_{wall}) in AlMePO-β, as a Function of Temperature, Obtained by Matching the ^{2}H NMR of d_6-Benzene

T/K	N_{iso}	N_{wall}
273	0.968	0.032
253	0.957	0.043
223	0.930	0.070
203	0.903	0.097
183	0.862	0.138
151	0.724	0.276
133	0.585	0.414

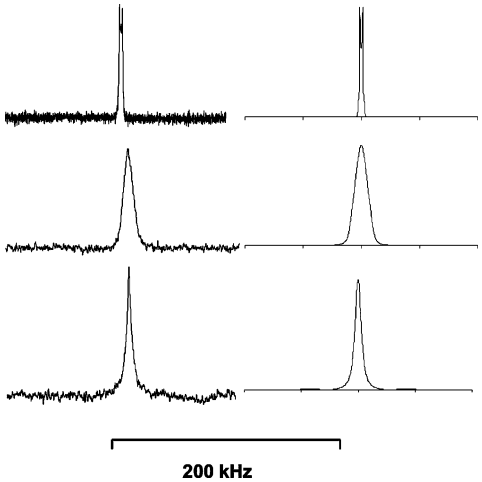

Figure 14. Experimental (left) and simulated (right) ^{2}H NMR spectra for benzene in AlMePO-β at (top) 253, (middle) 151, and (bottom) 133 K. Details of the simulation are given in the text.

Parallel simulation of the motion of benzene in the narrower channels of AlMePO-α predict more restricted reorientation: these simulations can be analyzed and used in the interpretation of the ^{2}H wide-line NMR spectra. The study of adsorbed benzene in these polymorphs emphasizes the power of a joint experimental and theoretical approach to establishing modes of adsorbate motion.

Denayer et al.[13] show that, for some zeolites, isopentane is observed to adsorb preferentially over *n*-pentane, which is the reverse of that expected on the grounds of the enthalpy of adsorption. This example of "inverse shape selectivity" is

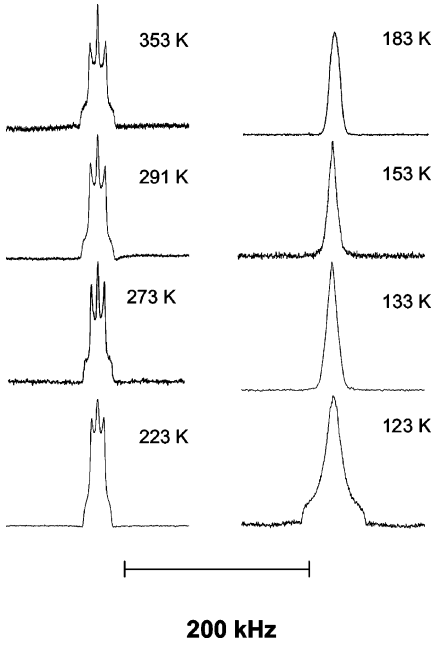

Figure 15. Variable-temperature quadrupole echo ^{2}H NMR of d_6-benzene adsorbed in AlMePO-α (with some unreacted AlMePO-β) at a loading of 4.5 wt %.

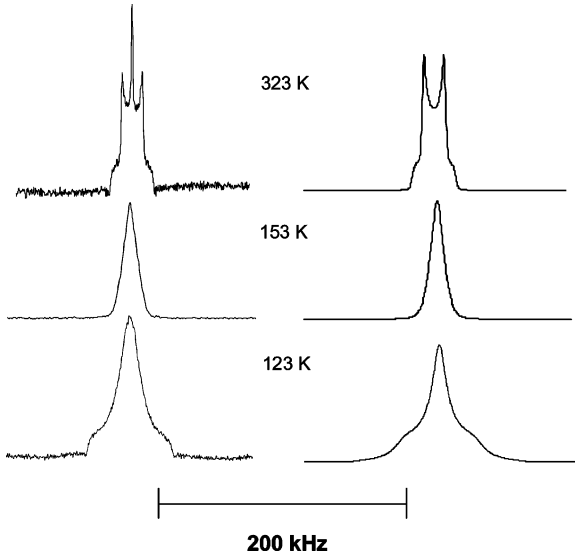

Figure 16. Experimental ^{2}H NMR spectra (left) of d_6-benzene in AlMePO-α at (top) 323, (middle) 153, and (bottom) 123 K. The simulated spectra (right) use a model in which the benzene undergoes C_6 rotation, $2\pi/3$ flips, and 30° out-of-plane motion.

explained in terms of the retention of rotational mobility of isopentane within the zeolite cages compared to *n*-pentane, which is not expected to rotate, and therefore has a more negative entropy of adsorption. For benzene in a mixture of AlMePOs, it would therefore be expected that benzene would adsorb preferentially into the β-polymorph, where it retains rotational entropy. This would explain the much higher ^{2}H signal attributed to benzene in the small amounts of untransformed β in the AlMePO-α than would be expected on the basis of solid state ^{31}P and powder XRD estimates of the relative amounts of the α- and β-polymorphs. A similar effect could explain the onset of 2-methylpropane adsorption occurring at lower partial pressures on AlMePO-β than on AlMePO-α as reported by Maeda et al.[7] Indeed, our preliminary ^{2}H NMR studies of adsorbed deuterated 2-methylpropane also indicate its higher mobility in the β-polymorph than in the α-polymorph. It may therefore be possible to achieve entropy-driven hydrocarbon separations using these two solids.

Conclusions

Variable-temperature quadrupole echo ^{2}H NMR has been performed on d_3,d_3-*p*-xylene, d_3-, d_5-, and d_8-toluenes, and d_6-benzene within the $Al_2(CH_3PO_3)_3$ polymorphs α and β. Although the pore structures of the two solids are very similar, the slightly different channel shapes (the cross section of AlMePO-α is markedly triangular) result in important differences in the spectra. The motion of d_3,d_3-*p*-xylene in both polymorphs, as interpreted from analysis of the ^{2}H NMR of the rapidly rotating CD_3 groups, is approximated by the molecule moving between different sites on a cone, the half-angle of which depends on the effective diameter of the pores. By this measure, which takes no account of deviations of the pore from a perfect cylinder, the pore sizes of β and α are estimated at 7.3 and 6.2 Å, respectively, which are slightly larger than the crystallographic estimates.

The ^{2}H NMR of toluene in these solids can in large part be simulated by again considering the para-axis to exchange between (at least) three sites on a cone, with the aromatic ring performing independent $2\pi/3$ flips. This is broadly in agreement with the motion that is predicted by molecular dynamics simulations. Signal from the aromatic ortho- and meta-deuterons of toluene in AlMePO-α is found to decrease in intensity as the temperature is decreased, suggesting that the rotational exchange occurs at an intermediate exchange rate at this temperature and adding further detail to the model.

Measurements on d_6-benzene adsorbed in the two polymorphs show the most striking differences. Although the change in structure between the two solids is small, the change in channel shape has a major effect on the motion of benzene. In the slightly more cylindrical channels of AlMePO-β, it is able to tumble freely, and it does this at all temperatures studied. As the temperature is lowered, it also spends some time at sites closer to the walls. The situation is very different in AlMePO-α, in the channels of which the benzene motion is strongly constrained. By combining ^{2}H NMR with molecular dynamics simulations, it appears that the strongly triangular shape prevents isotropic motion, restricting the benzene to flipping between three symmetry-related sites in the pores, with the plane of the aromatic ring approximately parallel to the channel axes. The observed line shape is matched most closely if additional motion due to the rotation of benzene around its C_6 axis and some out-of-plane motion are also included.

These results show the ability of the two closely similar microporous solids to differentiate strongly between aromatics on the basis of their size and shape. For the example of benzene adsorbed in AlMePO-β, the high observed mobility can be attributed to the rotating methyl groups lining the pores. Finally, the combination of ^{2}H NMR and MD appears to be a highly promising approach to enable ^{2}H NMR line shapes to be interpreted on the molecular scale with less ambiguity, and to offer a powerful tool to understanding the mobility of adsorbed molecules within new classes of microporous materials. Further research is ongoing to determine the relation of translational motion to reorientation mechanisms.

Acknowledgment. Professor Robert Vold (William and Mary College) kindly supplied the MXQET codes. We gratefully acknowledge the help of Dr. P. Wormald for assistance in collecting the ^{27}Al and ^{31}P NMR, and the EPSRC for financial assistance to J.G. and R.N.D.

Supporting Information Available: Additional XRD, ^{27}-Al MAS NMR, C_7H_8 adsorption isotherms, experimental and simulated ^{2}H NMR line shapes, and MXQET input files. This material is available free of charge via the Internet at http://pubs.acs.org.

References and Notes

(1) Eddaoudi, M.; Kim, J.; Rosi, N.; Vodak, D.; Wachter, J.; O'Keefe, M.; Yaghi, O. M. *Science* **2002**, *295*, 469. Chae, H. K.; Siberio-Perez, D. Y.; Kim, J.; Go, Y.; Eddaoudi, M.; Matzger, A. J.; O'Keeffe, M. *Nature* **2004**, *427*, 523.

(2) Férey, G.; Serre, C.; Mellot-Draznieks, C.; Millange, F.; Surblé, S.; Dutour, J.; Magiolaki, I. *Angew. Chem., Int. Ed.* **2004**, *43*, 6296.

(3) Bradshaw, D.; Claridge, J. B.; Cussen, E. J.; Prior, T. J.; Rosseinsky, M. J. *Acc. Chem. Res.* **2005**, *38*, 273.

(4) Maeda, K. *Microporous Mesoporous Mater*. **2004**, *73*, 47.

(5) Maeda, K.; Akimoto, J.; Kiyozumi, Y.; Mizukami, F. *Angew. Chem., Int. Ed. Engl.* **1995**, *34*, 1199.

(6) Maeda, K.; Akimoto, J.; Kiyozumi, Y.; Mizukami, F. *J. Chem. Soc., Chem. Commun.* **1995**, 1033.

(7) Maeda, K.; Kiyozumi, Y.; Mizukami, F. *J. Phys. Chem. B* **1997**, *101*, 4402.

(8) Schumacher, C.; Gonzalez, J.; Wright, P. A.; Seaton, N. A. *Phys. Chem. Chem. Phys.* **2005**, *7*, 2351.

(9) Eckman, R. R.; Vega, A. J. *J. Phys. Chem*. **1986**, *90*, 4679.

(10) Kustanovich, I.; Fraenkel, D.; Luz, Z.; Vega, S.; Zimmerman, H. *J. Phys. Chem*. **1988**, *92*, 4134.

(11) Kustanovich, I.; Vieth, H. M.; Luz, Z.; Vega, S. *J. Phys. Chem*. **1989**, *9*, 7427.

(12) Shantz, D. F.; Lobo, R. F. *Top. Catal*. **1999**, *9*, 1.

(13) Denayer, J. F. M.; Ocakoglu, R. A.; Arik, I. C.; Kirschhock, E. A.; Martens, J. A.; Baron, G. V. *Angew. Chem., Int. Ed.* **2005**, *44*, 400.

(14) Devi, R. N.; Edgar, M.; Gonzalez, J.; Slawin, A. M. Z.; Tunstall, D. P.; Grewal, P.; Cox, P. A.; Wright, P. A. *J. Phys. Chem. B* **2004**, *108*, 535.

(15) Ratcliffe, C. I.; Soldatov, D. V.; Ripmeester, J. A. *Microporous Mesoporous Mater*. **2004**, *73*, 71.

(16) Gonzalez, J.; Devi, R. N.; Tunstall, D. P.; Cox, P. A.; Wright, P. A. *Microporous Mesoporous Mater*. **2005**, *84*, 97.

(17) Greenfield, M. S.; Ronemus, A. D.; Vold, R. L.; Vold, R. R.; Ellis, P. D.; Raidy, E. *J. Magn. Reson.* **1987**, *72*, 89.

(18) Ok, J. H.; Vold, R. R.; Vold, R. L.; Etter, M. C. *J. Phys. Chem*. **1989**, *93*, 7618.

(19) Sato, T.; Kunimori, K.; Hayashi, S. *Phys. Chem. Chem. Phys*. **1999**, *1*, 3839.

(20) Jude, A. R.; Greathouse, D. V.; Leister, M. C.; Koeppe, R. E. *Biophys. J.* **1999**, *77*, 1927.

(21) Auerbach, S. M.; Bull, L. M.; Henson, N. J.; Metiu, H. I.; Cheetham, A. K. *J. Phys. Chem*. **1996**, *100*, 5923. Ramanan, H.; Auerbach, S. M.; Tsapatsis, M. *J. Phys. Chem. B* **2004**, *108*, 17171.

(22) Carter, V. J.; Wright, P. A.; Gale, J. D.; Morris, R. E.; Sastre, E.; Perez-Pariente, J. *J. Mater. Chem.* **1997**, *7*, 2287. Maeda, K.; Sasaki, A.; Watanabe, K.; Kiyozumi, Y.; Mizukami, F. *Chem. Lett.* **1997**, *9*, 879.

(23) Carter, V. J.; Kujanpaa, J.; Riddell, F. G.; Wright, P. A.; Turner, J. F. C.; Catlow, C. R. A.; Knight, K. S. *Chem. Phys. Lett.* **1999**, *313*, 505.

(24) Powell, J. C.; Phillips, W. D.; Melby, L. R.; Panar, M. *J. Chem. Phys*. **1965**, *43*, 3442.

(25) *Discover*, version 98.0; Accelrys: San Diego, CA.

(26) Grewal, P.; Wright, P. A.; Cox, P. A. Manuscript in preparation.